Electronic Supplementary Material (ESI) for RSC Advances.

This journal is © the Owner Societies 2020

Switching Xe/Kr adsorption Selectivity in the Modified SBMOF-1: A Theoretical Study

Jiao-jiao Qian,[a] Guang-hui Chen,[*a] Song-tao Xiao,[b] Hui-bo Li,[b] Ying-gen Ouyang,[b] Qiang Wang[c]

[a.] *epartment of Chemistry and Key Laboratory for Preparation and Application of Ordered Structural Materials of Guangdong Province, Shantou University, Guangdong515063, China. E-mail: ghchen@stu.edu.cn*

[b.] *Institute of Radiochemistry, China Institute of Atomic Energy (CIAE), Beijing, 102413, People's Republic of China.*

[c.] *Department of Applied Chemistry, College of Science, Nanjing Tech University, Nanjing 211816, People's Republic of China.*

Table S1. Crystal coordinate data of Mg-SBMOF-1.

	compound	Mg-SBMOF-1	
	crystal system	Monoclinic	
	space group	P21/N	
	a (Å)	11.8819	
	b (Å)	5.5555	
	c (Å)	22.6411	
	A (deg)	90.0000	
	β (deg)	101.3020	
	γ (deg)	90.0000	
coordinate information			
Mg	1.302877215	4.249901945	1.297709219
S	4.463027919	3.083191390	2.415803937
O	11.151640648	4.029404150	1.285942138
O	2.318243970	5.449334395	8.514926255
O	4.484505091	1.436818965	2.452215282
O	10.277164372	5.988829000	0.450479385
O	3.507131407	3.949904945	1.349217951
O	2.660195853	3.191690305	8.806883076
C	3.372922813	4.156125105	6.782279079
C	4.103405741	3.604741730	4.196185498
C	6.235770211	3.618019375	2.050358364
C	8.793321228	4.415566955	1.446462885
C	4.108354576	2.992747850	6.498981053
H	4.308918551	2.278643880	7.298032460
C	10.172437840	4.841784915	1.035725151
C	8.583839765	3.190801425	2.101645075
H	9.442911116	2.550696715	2.309678187
C	3.073110335	5.080171420	5.763427478
H	2.491449065	5.971106955	5.997881017
C	2.764021590	4.294845940	8.156585334
C	7.280351149	2.766139005	2.422908589
H	7.103917556	1.822092890	2.937107828
C	4.489737663	2.695250825	5.184620304
H	5.036762454	1.783148835	4.949278684
C	6.401736333	4.845673765	1.433363681
H	5.550547472	5.497945020	1.238207752
C	3.438501165	4.797396470	4.435745506
H	3.221800480	5.500056110	3.628257323
C	7.703705937	5.243058680	1.107215718
H	7.877060062	6.155160670	0.533515013

Table S2. modified force field parameters for MOF atoms.

atom	ε /k(KJ/mol)	σ (Å)	atom	ε /k(KJ/mol)	σ (Å)
Ca	0.24	3.40	Ti	0.07	2.83
Mg	0.46	2.69	Zn	0.52	2.46
Cd	0.95	2.54	Kr	1.38	3.64
Xe	1.84	4.10	S	1.44	3.59

Table S3. Adsorption Energies for Kr and Xe in X-SBMOF-1(X = Ca, Mg, Ti, Zn, Cd).

MOF	Q_{st}(KJ/mol)		E_{ads}(KJ/mol)	
	Kr	Xe	Kr	Xe
energy				
Mg-SBMOF-1	-24.25	-22.61	-28.53	-18.56
	-21.19[a] -0.09[b]	-19.58[a] -0.05[b]		
SBMOF-1	-27.21	-34.46	-30.21	-36.39
	-23.37[a] -0.86[b]	-29.32[a] -2.16[b]		
Zn-SBMOF-1	-25.86	-30.63	-29.86	-33.84
	-22.42[a] -0.47[b]	-26.61[a] -1.04[b]		
Cd-SBMOF-1	-26.24	-30.09	-28.24	-31.43
	-22.81[a] -0.45[b]	-26.23[a] -0.88[b]		
Ti-SBMOF-1	-13.61	-13.04	-14.91	-14.47
	-12.93[a] 0.00[b]	-12.81[a] 0.00[b]		

E_{ads} were calculated at GGA-PBE/DNP level.

a. represents the adsorption heat contributed by the host- guest interaction; b. represents the adsorption heat contributed by the host- guest interaction.

Table S4. Energy decomposition analysis of interaction between modified MOFs and Kr (unit: KJ/mol).

	S-F-2	S-CH_3-2	S-OH-2	S-NH_2-2	6NH_2-MgSBMOF-1
ΔE_{elec}	-0.57	-0.49	-0.58	-0.918	-0.75
percentage	3.5%	2.1%	3.4%	4.9%	3.5%
ΔE_{exc}	1.58	9.40	1.23	2.072	1.75
ΔE_{indu}	-8.40	-4.88	-7.34	-7.924	-10.36
percentage	51.1%	20.5%	42.5%	42.1%	48.0%
ΔE_{disp}	-7.47	-18.44	-9.34	-9.986	-10.48
percentage	45.4%	77.4%	54.1%	53.0%	48.5%
ΔE_{tot}	-14.86	-14.41	-16.03	-16.756	-19.83

ΔE_{elec}, ΔE_{exc}, ΔE_{indu}, ΔE_{disp}, ΔE_{tot} represent electrostatic interaction, exchange interaction, induction interaction, disperation interaction and total interaction respectively.

Figure Captions

Fig. S1 Unit cell structure diagram of X-SBMOF-1(X=Ca(a), Mg(b), Ti(c), Zn(d), Cd(e)) and SBMOF-1-Y (Y = -F(f), -CH3(g), -OH(h), -NH2(i)).

Fig. S2 Simulated (a) Xe and (b) Kr adsorption isotherm on SBMOF-1 along with the previously reported experimental data at 298 K.

Fig. S3(a) Energy-time curve of simulated annealing process by Forceite module;(b) Cell structure of Mg-SBMOF-1 after annealing simulation.

Fig. S4 The optimized single-substitution modified ligand SDB structure. Gray, red, dark blue, baby blue, yellow and white balls denote C, O, N, F, S, H atoms respectively.

Fig. S5 Calculated ground cavity diameter (GCD), pore limiting diameter (PLD) and largest cavity diameter (LCD) of single substitution modified Mg-SBMOF-1.

Fig. S6 Electrostatic potential map of single substitution modified Mg-SBMOF-1, (a) Mg-SBMOF-1; (b) 2-F-Mg-SBMOF-1; (c) 2-CH_3-Mg-SBMOF-1; (d) 2-OH-Mg-SBMOF-1; (e) 2-NH_2-Mg-SBMOF-1.

Fig. S7 Structure of organic ligand modified by amino poly-substitution.

Fig. S8 Simulated unary (a) Xe, (b) Kr adsorption isotherms on Mg-SBMOF-1 modified by -NH_2 with various number at deferent position with GCMC; (c) Calculated ground cavity diameter (GCD), pore limiting diameter (PLD) and largest cavity diameter (LCD) of double or multiple -NH_2 modified Mg-SBMOF-1; (d) Calculated unary Kr adsorption isotherms and polarizability on Mg-SBMOF-1 modified by -NH_2 with various number at deferent position with GCMC.

Fig. S9 The calculated Xe and Kr adsorption sites in SBMOF-1 at B3LYP/6-31+G(d)/SDD level.

Fig. S10 Intermolecular interactions (iso-surfaces: 0.005 a.u.) for different models using IGM analysis. (a) SBMOF-1 based host Xe; (b) SBMOF-1 based host Kr. All iso-surfaces are colored according to a BGR (blue-green-red, blue represents a strong attraction, green represents Vdw interaction, red denotes a strong repulsion) scheme over the electron density range $-0.05 < \rho(r) < 0.05$ a.u.

Fig. S11 (a)Simulated adsorption selectivity of Mg-SBMOF-1 for Kr/Xe at different molar fractions with GCMC; simulated the different molar ratios binary mixtures (Kr/Xe) isotherms with various temperature (b) 243 K; (c) 263K; (d) 298 K; (e) 313 K.

Fig. S1

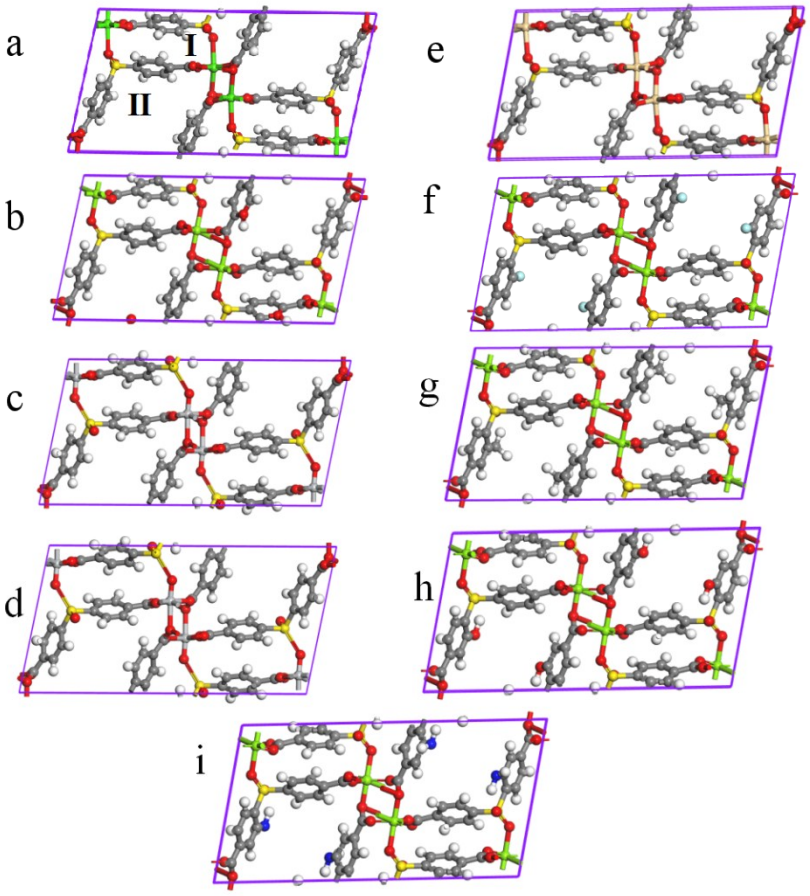

Fig. S2

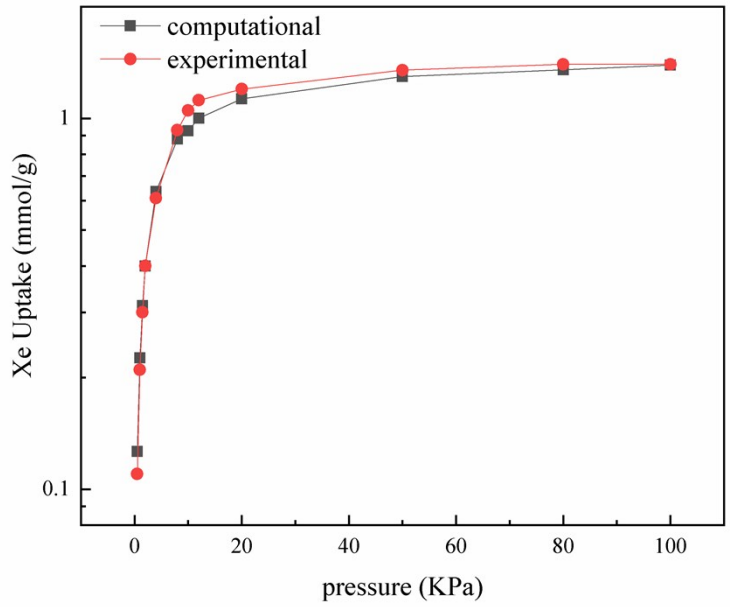
computational
experimental
Xe Uptake (mmol/g)
1
0.1
0
20
40
60
80
100
pressure (KPa)

(a)

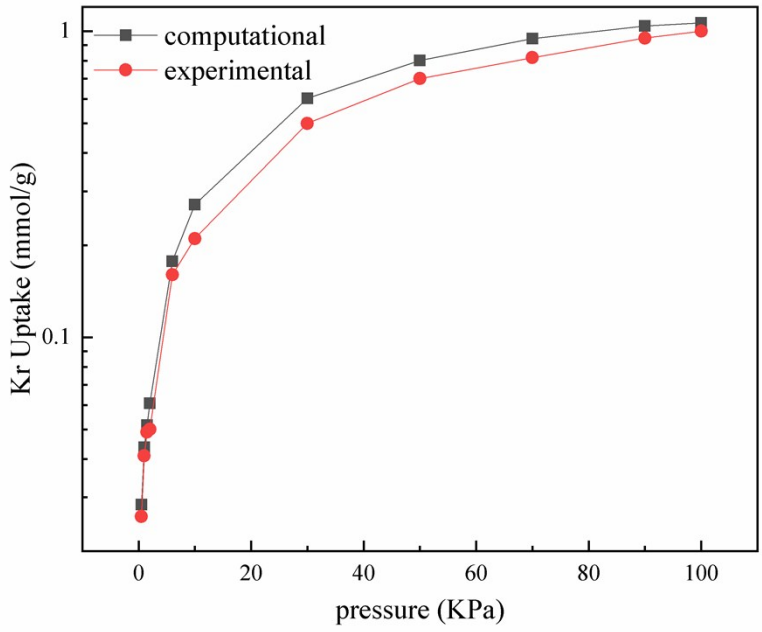
computational
experimental
Kr Uptake (mmol/g)
1
0.1
0
20
40
60
80
100
pressure (KPa)

(b)

Fig. S3

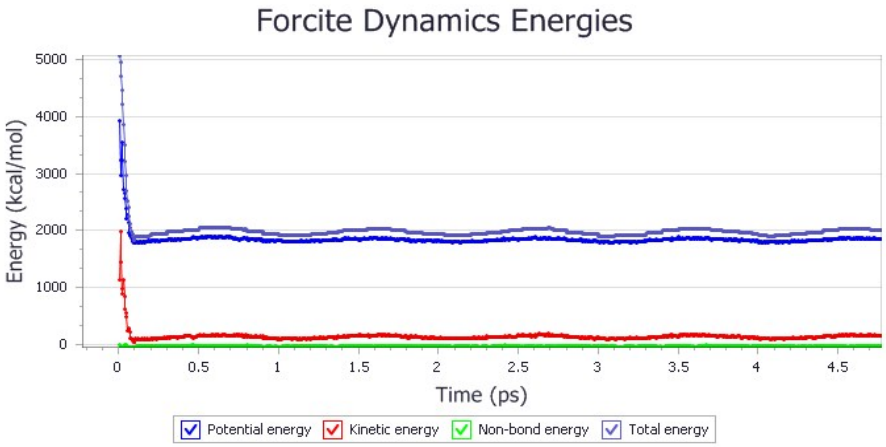
Forcite Dynamics Energies
Energy (kcal/mol)
5000
4000
3000
2000
1000
0
0
0.5
1
1.5
2
2.5
3
3.5
4
4.5
Time (ps)
Potential energy
Kinetic energy
Non-bond energy
Total energy

(a)

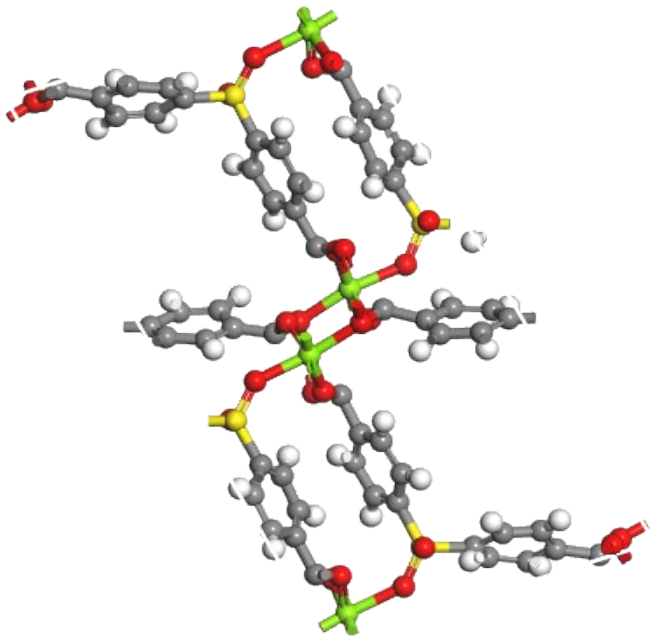

(b)

Fig. S4

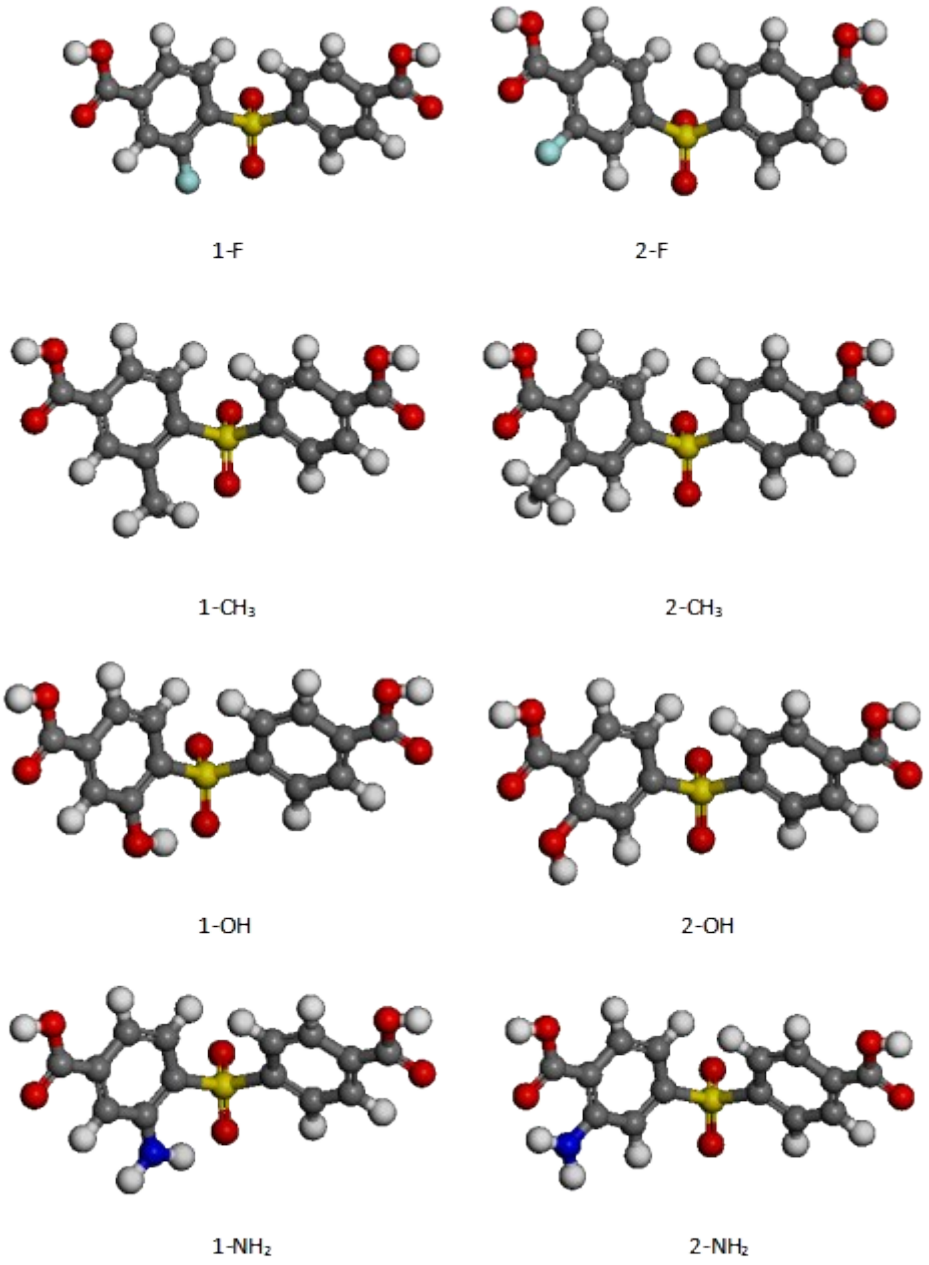

Fig. S5

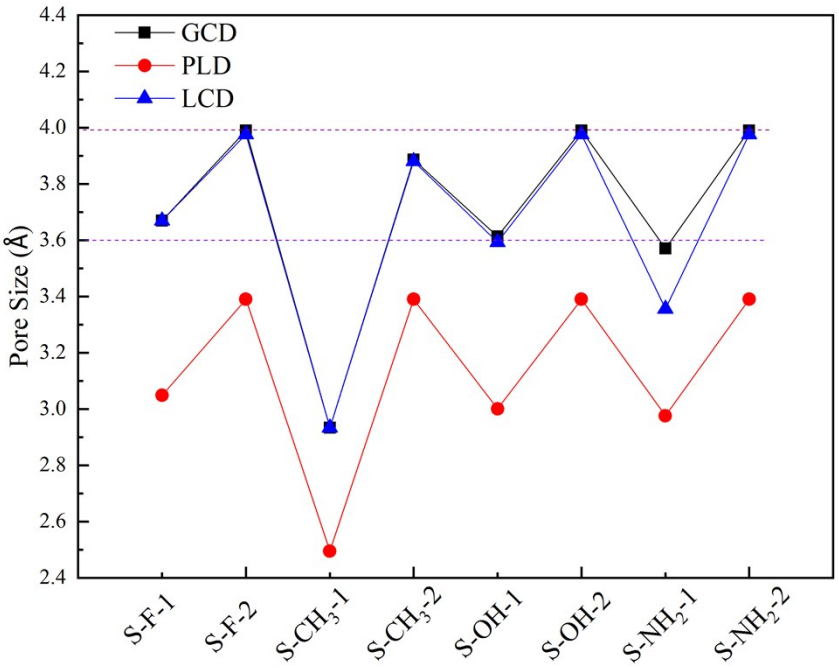
GCD
PLD
LCD
Pore Size (Å)
4.4
4.2
4.0
3.8
3.6
3.4
3.2
3.0
2.8
2.6
2.4
S-F-1
S-F-2
S-CH3-1
S-CH3-2
S-OH-1
S-OH-2
S-NH2-1
S-NH2-2

Fig. S6

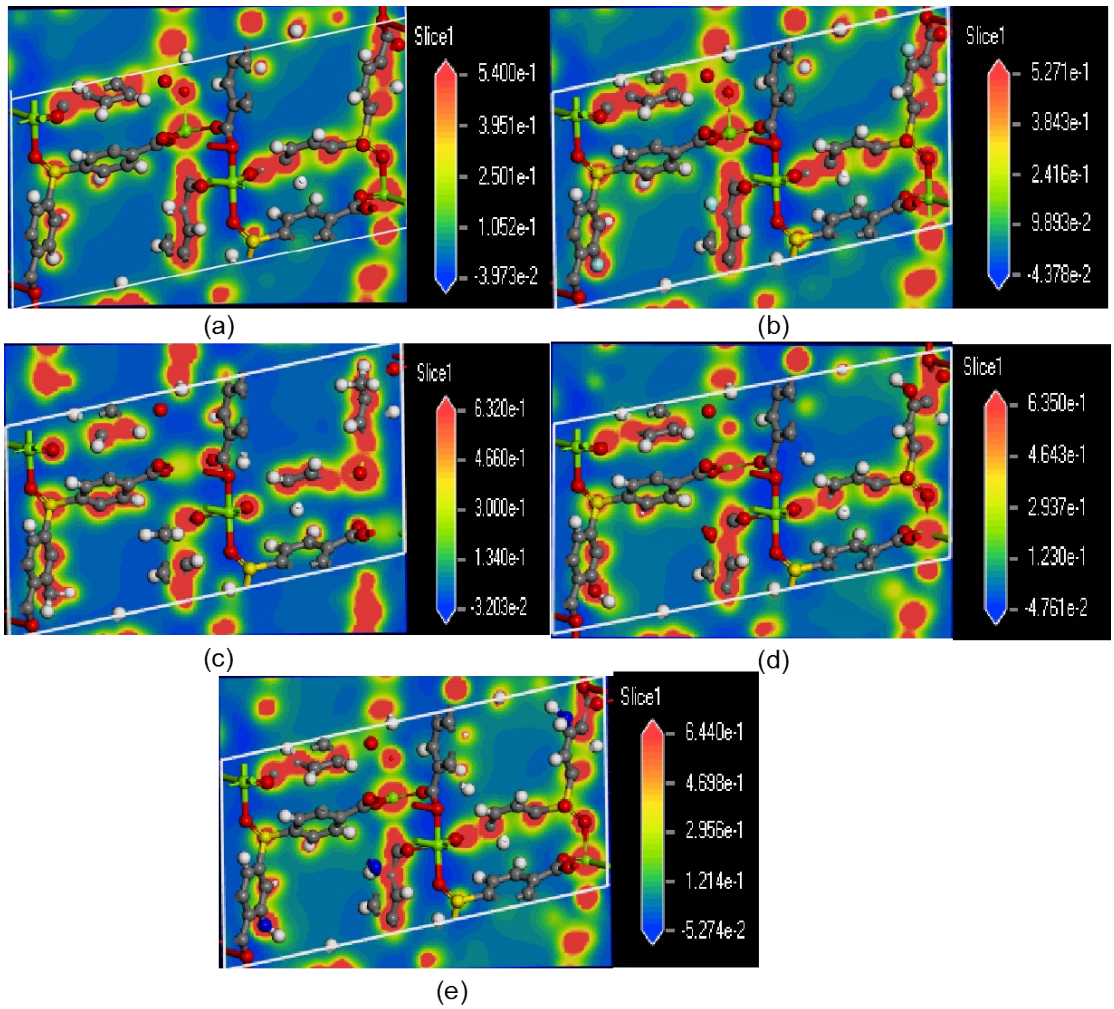
Slice1
5.400e-1
3.951e-1
2.501e-1
1.052e-1
-3.973e-2
(a)
Slice1
5.271e-1
3.843e-1
2.416e-1
9.893e-2
-4.378e-2
(b)
Slice1
6.320e-1
4.660e-1
3.000e-1
1.340e-1
-3.203e-2
(c)
Slice1
6.350e-1
4.643e-1
2.937e-1
1.230e-1
-4.761e-2
(d)
Slice1
6.440e-1
4.698e-1
2.956e-1
1.214e-1
-5.274e-2
(e)

Fig. S7

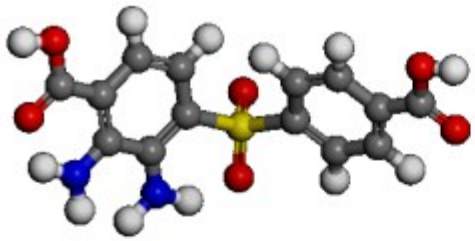

D-NH_2-1

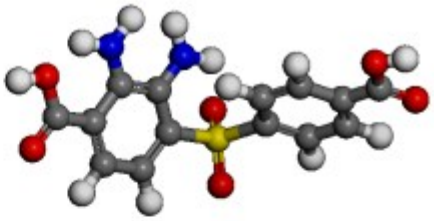

D-NH_2-2

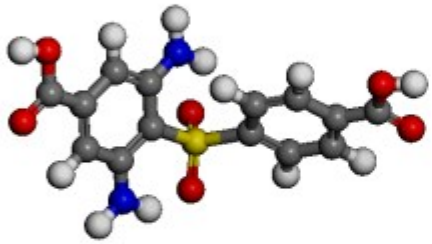

D-NH_2-3

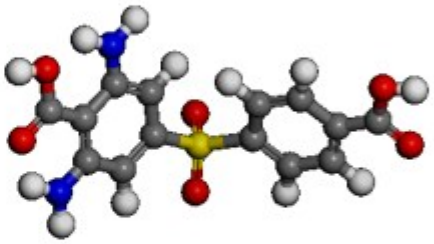

D-NH_2-4

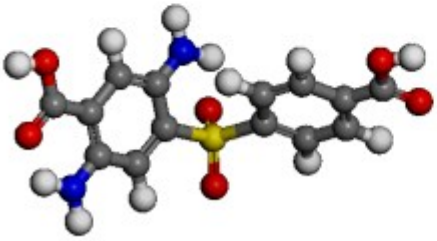

D-NH_2-5

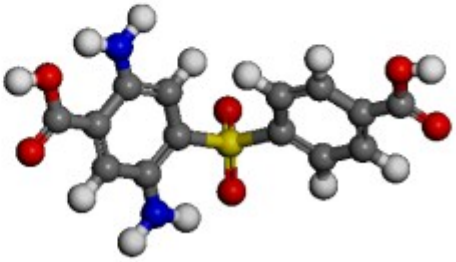

D-NH_2-6

Fig. S8

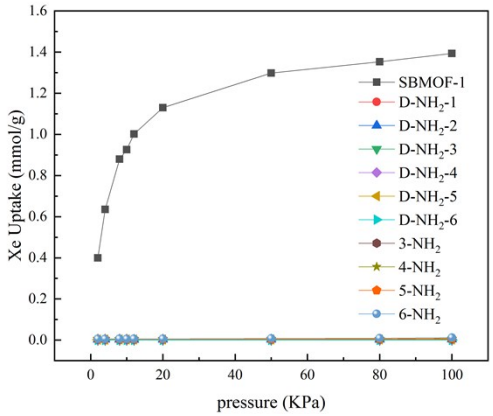
Xe Uptake (mmol/g)
pressure (KPa)
SBMOF-1
D-NH2-1
D-NH2-2
D-NH2-3
D-NH2-4
D-NH2-5
D-NH2-6
3-NH2
4-NH2
5-NH2
6-NH2

(a)

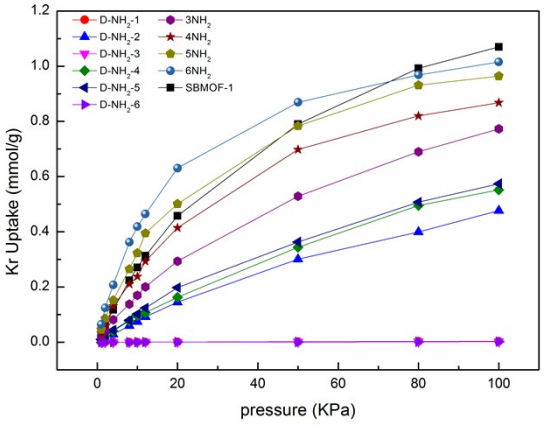
Kr Uptake (mmol/g)
pressure (KPa)
D-NH2-1
D-NH2-2
D-NH2-3
D-NH2-4
D-NH2-5
D-NH2-6
3NH2
4NH2
5NH2
6NH2
SBMOF-1

(b)

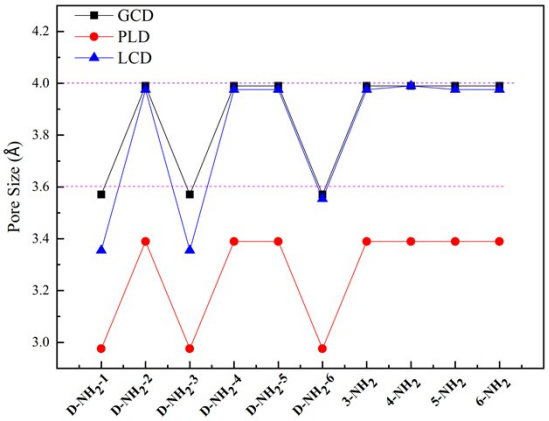
GCD
PLD
LCD
Pore Size (Å)
D-NH2-1
D-NH2-2
D-NH2-3
D-NH2-4
D-NH2-5
D-NH2-6
3-NH2
4-NH2
5-NH2
6-NH2

(c)

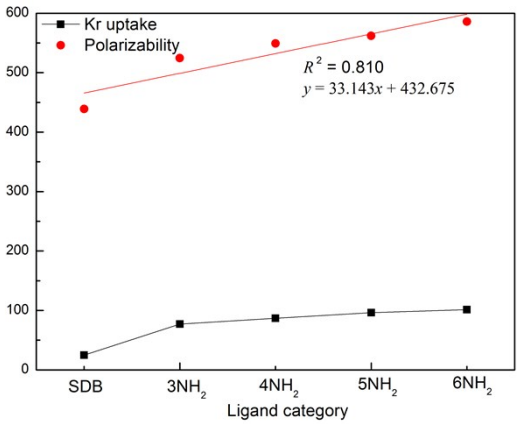
Kr uptake
Polarizability
R2 = 0.810
y = 33.143x + 432.675
SDB
3NH2
4NH2
5NH2
6NH2
Ligand category

(d)

Fig. S9

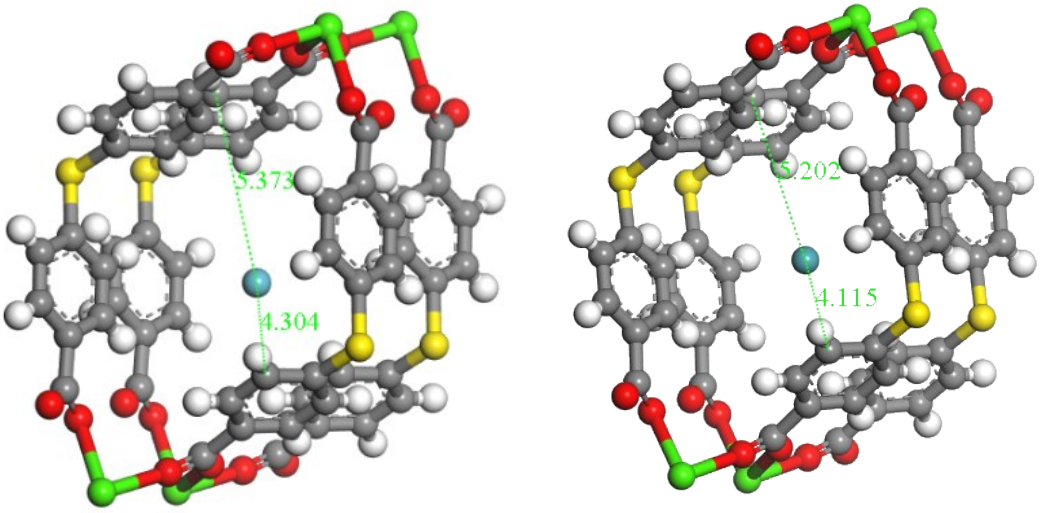

(a) (b)

Fig. S10

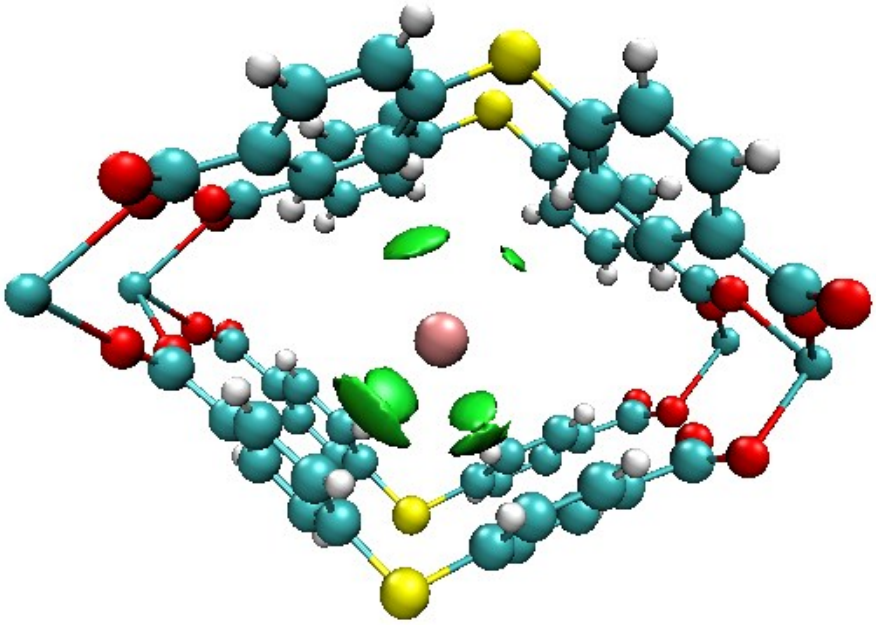

(a)

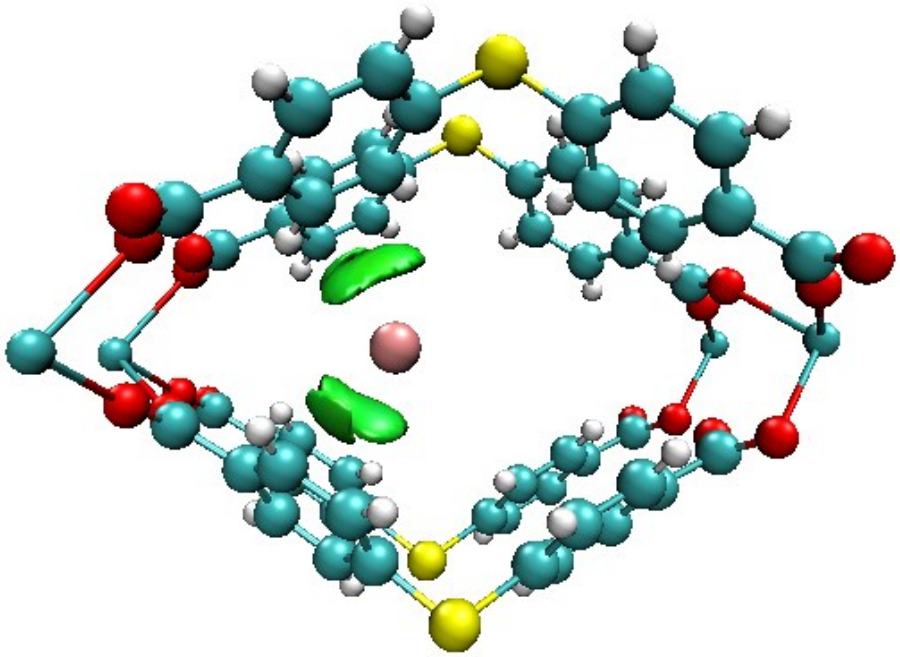

(b)

Fig. S11

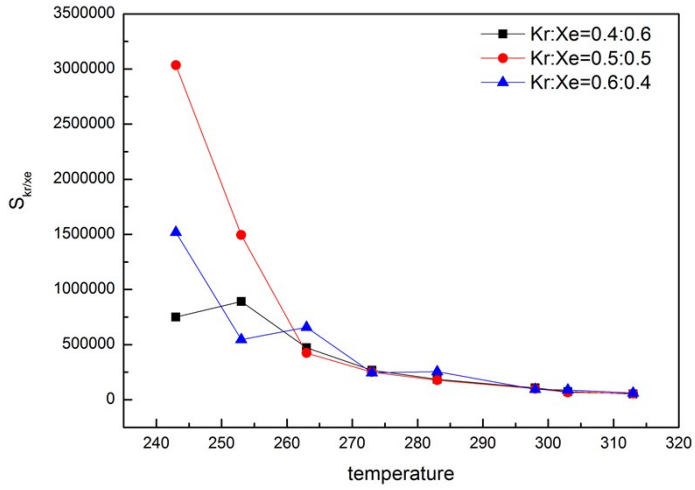

(a)

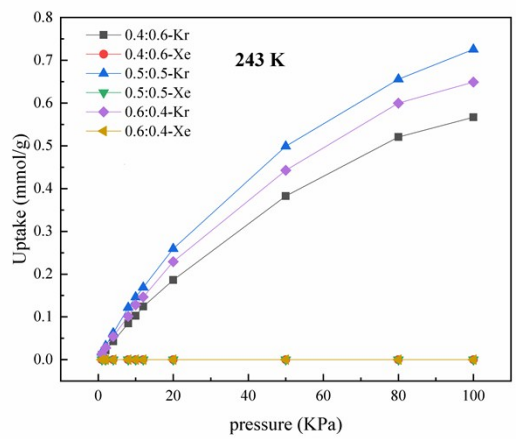

(b)

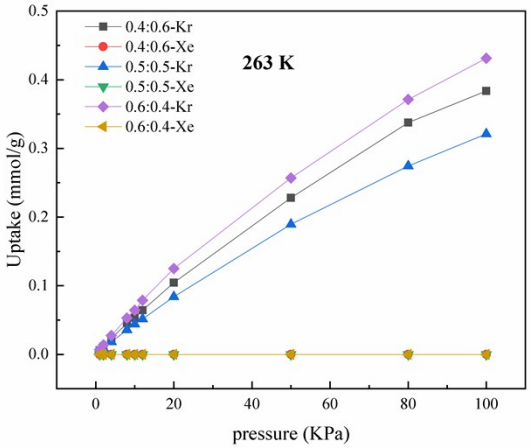

(c)

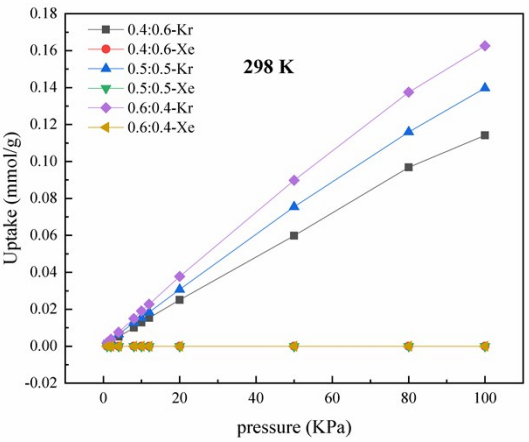

(d)

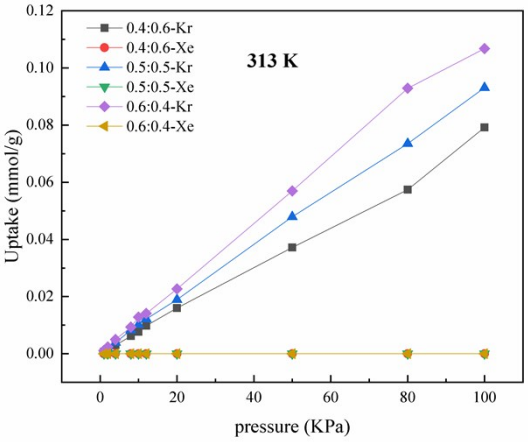

(e)